Optical and Quantum Electronics **33:** 1077–1087, 2001.

All-optical serial-to-parallel conversion of T-bits/s signals using a four-wave-mixing process

K. EMA[1]*, J. ISHI[1], H. KUNUGITA[1], T. BAN[2] AND T. KONDO[2]
[1]*Department of Physics, Sophia University, 7-1 Kioi-cho, Chiyoda-ku, Tokyo 102-8554, Japan*
[2]*Department of Material Science, The University of Tokyo, 7-3-1 Hongo, Bunkyo-ku, Tokyo 113-8656, Japan*
*(*author for correspondence, E-mail: k-ema@sophia.ac.jp)*

Received 4 October 2000; accepted 13 November 2000

Abstract. We report a simple method of a serial-to-parallel conversion that does not use a Fourier-transform system. The method is based on directly picking up a narrow temporal range of the skewed input signal by using a nonlinear wave mixing with the reference pulse. We show theoretically that the pick-up method is less influenced by the relaxation times of the nonlinear material. We demonstrate our method experimentally using a self-organized quantum-well material, and confirm that T-bits/s pulses are clearly converted into spatial patterns with conversion rates of 140 GHz.

Key words: serial-to-parallel conversion, four-wave-mixing process, self-organized quantum-well material

1. Introduction

Recent development of all-optical space–time-conversion techniques of ultrafast pulses (Ema 1991; Ema *et al.* 1991, 1992; Nuss *et al.* 1994; Sun *et al.* 1995, 1997; Mazurenko *et al.* 1996; Kan'an and Weiner 1998; Konishi and Ichioka 1999; Leaird and Weiner 1999; Marom *et al.* 1999) opens the possibility of ultrahigh bit-rate optical communication. In essence the technique of all-optical space-to-time (or parallel-to-serial) conversion is an expansion of real-time pulse-shaping technique (Ema 1991; Weiner *et al.* 1992; Weiner 2000). While the technique of all-optical time-to-space (or serial-to-parallel) conversion is based on the exchange of information between the spatial and the temporal channels using three-wave-mixing (TWM) (Ema *et al.* 1992; Mazurenko *et al.* 1996; Sun *et al.* 1997; Kan'an and Weiner 1998) or four-wave-mixing (FWM) (Ema 1991; Ema *et al.* 1991, 1992; Nuss *et al.* 1994; Sun *et al.* 1995; Marom *et al.* 1999) processes. The performance of the time-to-space conversion is thus determined by the nonlinear wave-mixing mechanism. In many cases FWM process is more desirable because it permits both space-to-time (Ema 1991; Sun *et al.* 1995; Marom *et al.* 1999) and time-to-space (Ema 1991; Ema *et al.* 1991; Nuss *et al.* 1994; Sun *et al.* 1995) conversion and has the possibility of cascade operation. However, there is a key problem associated with $\chi^{(3)}$ nonlinear materials; that is a trade-off

relation between a fast response and a high efficiency. In order to break this problem several nonlinear processes have been proposed and demonstrated. Excitonic large $\chi^{(3)}$ nonlinearity (Ema *et al.* 1991) and cascaded second-order nonlinearity (CSN) (Marom *et al.* 1999) are good candidates for ultrafast FWM space–time processing. One of the authors has demonstrated a time-to-space conversion with a fast response time of up to 13 ps using the giant excitonic $\chi^{(3)}$ in ZnSe film (Ema *et al.* 1991). However, the performance was achieved only at low temperature, because the giant excitonic nonlinearity smears out at room temperature.

Quite recently (Ishi *et al.* 2000) we have demonstrated a room-temperature operation of serial-to-parallel conversion using an excitonic resonant FWM process in an inorganic–organic self-organized quantum-well material $(C_6H_{13}NH_3)_2PbI_4$. Excitons in this material are very stable even at room temperature (Ishihara 1995), which leads to a large excitonic $\chi^{(3)}$ and a fast response time (Ishi *et al.* 1998; Kondo *et al.* 1998). The principle of our serial-to-parallel conversion is quite simple. It is based on a pick-up method that does not use a precise Fourier transformation. In this paper, we present the details of the pick-up method and discuss the influence of the relaxation times of the nonlinear material on the performance of the time-to-space conversion. We confirm theoretically and experimentally that our system can convert T-bits/s signals into clear spatial patterns with a conversion rate of at least 140 GHz.

2. Serial-to-parallel conversion by a pick-up method

The principle of our serial-to-parallel conversion is schematically shown in Fig. 1. Let the input-signal field $E_s(t,x)$ just before a grating have a temporal shape $U_s(t)$ and a spatial pattern $R_s(x)$ where x is the spatial coordinate perpendicular to the propagation direction of the signal. When the spectral width $\Delta\omega$ of the input-signal field is much smaller than the carrier frequency ω_0 ($\Delta\omega \ll \omega_0$), the pulse just after diffraction by the grating has a skewed shape of form (Marinez 1986; Shimizu 1987)

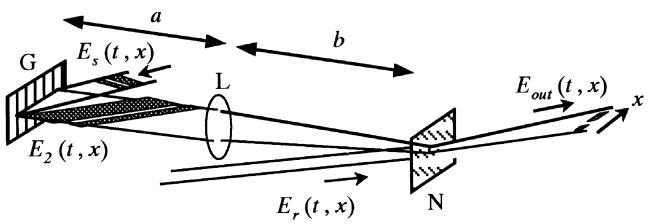

Fig. 1. Schematic illustration of our serial-to-parallel conversion. The temporal and spatial shapes of the pulses are shown as shaded areas. G, L and N are a grating, a lens and a nonlinear material, respectively.

$$E_2(t,x) \propto U_s(t-\alpha x)R_s(sx). \tag{1}$$

The parameters α and s are functions of the incident (θ_i) and diffraction (θ_o) angles;

$$\alpha = \frac{1}{c}\frac{\lambda}{d\cos\theta_o}, \quad s = \frac{\cos\theta_i}{\cos\theta_o} \tag{2}$$

where d is the groove period of the grating and c the velocity of light. In the standard approach, E_2 is then spatially Fourier-transformed to obtain a spectrally decomposed wave (SDW) of the signal field E_s. However, when E_s is real (i.e. the input signal has no phase modulation) and only the amplitude $|U_s(t)|^2$ is required as in the present case, a Fourier-transformation becomes superfluous. The x dependence of $E_2(t,x)$ at a fixed time is similar to the temporal shape of the input pulse; we thus can obtain the spatial pattern corresponding to the temporal shape of $E_s(t,x)$ by picking up a narrow temporal range of $E_2(t,x)$. In principle, this can be achieved by using an FWM process with a sufficiently short reference pulse in a nonlinear material inserted into the beam just after the grating. An actual system, however, always requires a certain distance between grating and nonlinear material. Moreover one would want to focus the field onto the nonlinear material with the help of a lens in order to increase intensity. Fortunately there is no need to worry that the generated spatial pattern from the FWM process depends greatly on the relative position of grating, lens and nonlinear material. We will shortly show that the spatial pattern of the FWM field does not depend on where the FWM occurs, and always corresponds to the spatial version of the input temporal shape.

After propagating distances a (before lens) and b (after lens), the field $E_3(t,x)$ on the nonlinear material becomes

$$E_3(t,x) = \sqrt{\frac{fl}{\lambda(a+l)b^2}}\exp\left[i\frac{\pi}{\lambda b}x^2\left(1-\frac{al}{b(a+l)}\right)\right] \times [\tilde{E}_2(t,\beta x)\otimes H(\beta x)] \tag{3}$$

where $\tilde{E}_2(t,x)$ represents the spatial Fourier-transformation of $E_2(t,x)$, f is the focal length of the lens, $\otimes$ means convolution, and β, l, and $H(k)$ are defined by

$$\beta = \frac{l}{a+l}\frac{2\pi}{\lambda b}, \quad \frac{1}{l} = \frac{1}{b} - \frac{1}{f} \tag{4}$$

$$H(k) = \frac{1}{2\pi}\sqrt{\lambda(a+l)}\exp\left[-i\frac{\lambda(a+l)}{4\pi}k^2\right]. \tag{5}$$

When the spatial extent of $R_s(x)$, X, is much larger than the corresponding temporal extent of $U_s(t)$, T, (i.e. $\alpha X \gg T$), $E_3(t,x)$ becomes

$$E_3(t,x) \propto \exp\left[\mathrm{i}\frac{\pi}{\lambda b}x^2\left(1-\frac{al}{b(a+l)}\right)\right] \times \left[\tilde{U}^*\left(\frac{\beta}{\alpha}x\right)\exp\left(-\mathrm{i}\frac{\beta}{\alpha}xt\right) \otimes H(\beta x)\right] \tag{6}$$

where $\tilde{U}(\omega)$ represents the temporal Fourier transform of $U(t)$. The quadratic phase modulation factor in Equation (6) can be ignored, if

$$\left|\frac{\pi}{\lambda b}\left(1-\frac{al}{b(a+l)}\right)\right| \ll \left(\frac{\beta}{\alpha}T\right)^2 \tag{7}$$

is satisfied. This inequality is easily transformed into

$$\left|\frac{\Delta a}{f}\right| \ll \left(\frac{T}{\alpha}\right)^2 \frac{4\pi}{\lambda f}, \tag{8}$$

where $\Delta a = f - a$. When T is of the order of picoseconds or subpicoseconds, the right side in Equation (8) is approximately of order 10^0 to 10^2. In this case we can drop the quadratic phase modulation factor. For a precise Fourier-transform system ($a = b = f$, thus $l \to \infty$), $E_3(t,x)$ becomes a complete SDW of $E_s(t,x)$

$$E_3(t,x) \propto \tilde{U}^*\left(\frac{2\pi}{\alpha\lambda f}x\right)\exp\left(-\mathrm{i}\frac{2\pi}{\alpha\lambda f}xt\right). \tag{9}$$

In the FWM process, $E_3(t,x)$ is mixed with the reference field $E_r(t,x) = U_r(t)R_r(x)$ and the generated FWM field $E_4(t,x)$ is given by

$$E_4(t,x) \propto \chi^{(3)}E_r(t,x)^2E_3^*(t,x) \tag{10}$$

$$\propto U_r^2(t) \times \left[\tilde{U}\left(\frac{\beta}{\alpha}x\right)\exp\left(\mathrm{i}\frac{\beta}{\alpha}xt\right) \otimes H^*(\beta x)\right] \tag{11}$$

where we assume that the response of the nonlinear material is instantaneous (i.e. $\chi^{(3)} = \text{const}$) and the extent of $R_r(x)$ is sufficiently large. Then the Fourier-transformed or infinite far field of $E_4(t,x)$ becomes

$$E_{\text{out}}(t,x) \propto \int E_4(t,x')\exp(-\mathrm{i}\eta x'x)\mathrm{d}x'$$

$$\propto U_r^2(t)U_s(t-(\eta/\beta)\alpha x)h((\eta/\beta)x) \tag{12}$$

where $h(x)$ represents the Fourier transform of $H(k)$ and η is $2\pi/\lambda f$. Since $h(x)$ is just a phase function, it does not affect the pattern of $|E_{\text{out}}(t,x)|^2$. Of course the absolute intensity of $|E_{\text{out}}(t,x)|^2$ depends on the position of the nonlinear material. Actually only the time integrated intensity can be observed. It is the form of

$$I_{\text{out}}(x) \propto \int |U_{\text{r}}(t)|^4 |U_{\text{s}}(t - (\eta/\beta)\alpha x)|^2 \, \mathrm{d}t. \tag{13}$$

$I_{\text{out}}(x)$ is proportional to the cross-correlation of $|U_{\text{s}}(t)|^2$ with $|U_{\text{r}}(t)|^4$, and does not depend on the relative position among grating, lens and nonlinear material. In an actual system, the finite extent of $R_{\text{s}}(x)$ and $R_{\text{r}}(x)$ limit the time window and the spatial resolution of the conversion, respectively.

3. Influence of the relaxation times of the nonlinear material

With a resonant nonlinearity we have to consider relaxation times of the material. The converted spatial pattern has a tail along x due to the transverse relaxation time T_2 and possibly the longitudinal relaxation time T_1. This decreases the resolution of the spatial patterns. In order to consider this problem quantitatively, we have to calculate the frequency components of the FWM field using a frequency-dependent susceptibility $\chi^{(3)}(\omega;\omega_1,\omega_2,\omega_3)$. For simplicity we assume that $E_3(t,x)$ is in the Fourier-transform case (Equation (9)). The frequency components of $E_3(t,x)$ and $E_{\text{r}}(t,x)$ are then given by

$$E_3(\omega,x) \propto \tilde{U}^*\left(\frac{2\pi}{\alpha\lambda f}x\right)\delta\left(\omega - \frac{2\pi}{\alpha\lambda f}x\right), \tag{14}$$

$$E_{\text{r}}(\omega,x) \propto \tilde{U}_{\text{r}}(\omega) \tag{15}$$

and $E_4(t,x)$ becomes (Butcher and Cotter 1990)

$$\begin{aligned} E_4(\omega,x) &= \int \mathrm{d}\omega_1 \int \mathrm{d}\omega_2 \chi^{(3)}(\omega;\omega_1,\omega_2,\omega_3) E_{\text{r}}(\omega_1) E_{\text{r}}(\omega_2) E_3^*(\omega_3) \\ &\propto U_{\text{s}}\left(\frac{2\pi}{\alpha\lambda f}x\right) \int \mathrm{d}\omega_1 \int \mathrm{d}\omega_2 \chi^{(3)}(\omega;\omega_1,\omega_2,\omega_3) \tilde{U}_{\text{r}}(\omega_1)\tilde{U}_{\text{r}}(\omega_2) \\ &\quad \times \delta\left(\omega_3 - \frac{2\pi}{\alpha\lambda f}x\right) \end{aligned} \tag{16}$$

where $\omega_1 + \omega_2 - \omega_3 = \omega$. The information of the relaxation times T_1 and T_2 is included in the frequency dependence of $\chi^{(3)}(\omega;\omega_1,\omega_2,\omega_3)$. The frequency component of $E_{\text{out}}(t,x)$ is thus given by

$$E_{\text{out}}(\omega,x) \propto \int E_4(\omega,x')\exp\left(-\mathrm{i}\frac{2\pi}{\lambda f}x'x\right)\mathrm{d}x'$$
$$\propto \int \mathrm{d}\omega_1 \int \mathrm{d}\omega_2 \chi^{(3)}(\omega;\omega_1,\omega_2,\omega_3)\tilde{U}_{\text{r}}(\omega_1)\tilde{U}_{\text{r}}(\omega_2)\tilde{U}_{\text{s}}(\omega_3)$$
$$\times \exp(-\mathrm{i}\alpha x\omega_3). \tag{17}$$

The last formula is exactly equal to that of a two-pulse time-integrated FWM signal if αx is replaced by time delay τ. Since a two-pulse time-integrated FWM signal decays with time constant T_2, the converted spatial pattern has a tail along x corresponding to T_2. Fig. 2 (solid lines) shows the calculated dependence of T_1 and T_2 on the spatial patterns when two 500-fs pulses separated by 1 ps are converted. In this calculation we used $\chi^{(3)}(\omega;\omega_1, \omega_2,\omega_3)$ of a simple two-level model (Boyd 1992). As shown in Fig. 2, the spatial patterns depend on only T_2 in the present pick-up method.

In the standard method, the reference pulse is also Fourier-transformed by a grating and a lens to produce its SDW, and this SDW is then used to compensate the phase factor of $E_3(t,x)$ in the wave-mixing process. In this case, the frequency-dependent response of the nonlinear material produces a position-dependent response in the Fourier plane, which leads to an undesirable wave mixing between the temporal and spatial channels. $E_{\text{out}}(t,x)$ in this case is given by

$$E_{\text{out}}(t,x) \propto \int \mathrm{d}x' \tilde{U}_{\text{r}}^2\left(\frac{\pi}{\alpha\lambda f}x'\right)\tilde{U}_{\text{s}}\left(\frac{2\pi}{\alpha\lambda f}x'\right)$$
$$\times \chi^{(3)}\left(\omega_0+\frac{\pi}{\alpha\lambda f}x', \omega_0+\frac{\pi}{\alpha\lambda f}x', \omega_0+\frac{2\pi}{\alpha\lambda f}x'\right)$$
$$\times \exp\left(-\mathrm{i}\frac{2\pi}{\lambda f}x'x\right). \tag{18}$$

Fig. 2 (dashed line) shows the calculated spatial patterns in the standard method. In this case T_1 as well as T_2 influence the spatial pattern of the time-to-space conversion.

In the serial-to-parallel conversion system of the pick-up method, only T_2 limits the maximum convertible bit rate of the input signal. The longitudinal relaxation time T_1 limits the repetition rate of the conversion, because a large T_1 causes undesirable FWM processes between the reference field and the preceding signal field.

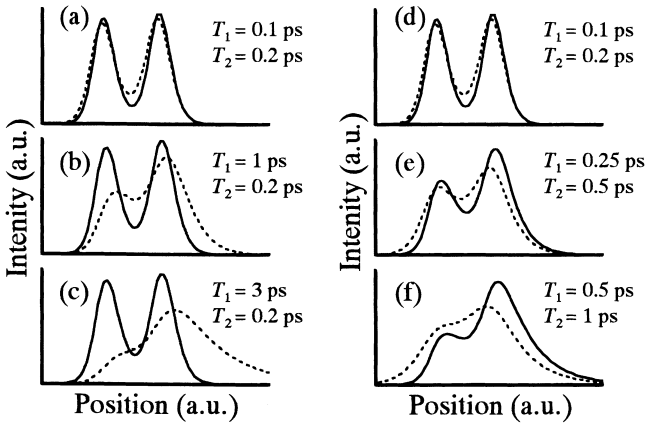

Fig. 2. Calculated influence of T_1 and T_2 on spatial patterns when two 500-fs pulses separated by 1 ps are converted in the pick-up method (solid lines) and the Fourier-transform method (dashed line). The left side of the figure ((a)–(c)) shows that the dependence of T_1 when T_2 is fixed to 0.2 ps. The right side of the figure ((d)–(e)) shows that the dependence of T_2 when T_1 is fixed to $T_1 = T_2/2$.

4. Self-organized quantum-well material

For an experimental demonstration we use an inorganic-organic-layered perovskite-type material $(C_6H_{13}NH_3)_2PbI_4$. This is a self-organized quantum-well material in which inorganic well layers are composed of a two-dimensional network of corner-sharing $[PbI_6]^{4-}$ octahedra contained between organic barrier layers of alkylammonium chains (Ishihara 1995). Since the dielectric constant of the barrier layer is much lower than that of the well layer, excitons are tightly confined in the inorganic well layers not only due to the quantum confinement effect but also due to the dielectric confinement effect (Hanamura *et al.* 1988). Consequently, the excitons have an extremely large binding energy ($\simeq$400 meV) and a large oscillator strength ($\simeq$0.7 per formula unit) (Ishihara 1995; Hanamura *et al.* 1988). The absorption spectrum of the excitons at room temperature is shown in Fig. 3. We have recently shown that $\chi^{(3)}(\omega;\omega,-\omega,\omega)$ of $(C_6H_{13}NH_3)_2PbI_4$ at the exciton resonance is as large as $\simeq 10^{-6}$ esu (Kondo *et al.* 1998) at room temperature, and that the longitudinal and transverse relaxation times T_1, T_2 at low temperature are approximately 7 and 0.5 ps, respectively (Ishi *et al.* 1998; Kondo *et al.* 1998). The relaxation times at room temperature are thus estimated that $T_1 < 7$ ps and $T_2 < 0.5$ ps. Therefore the resolution of the spatial pattern can be expected to be the same as shown in Fig. 2(c).

The samples used in our experiment were 100 nm-thick polycrystalline films spin-coated on optically flat glass substrates. The films were highly oriented with the inorganic well layers parallel to the substrate surface.

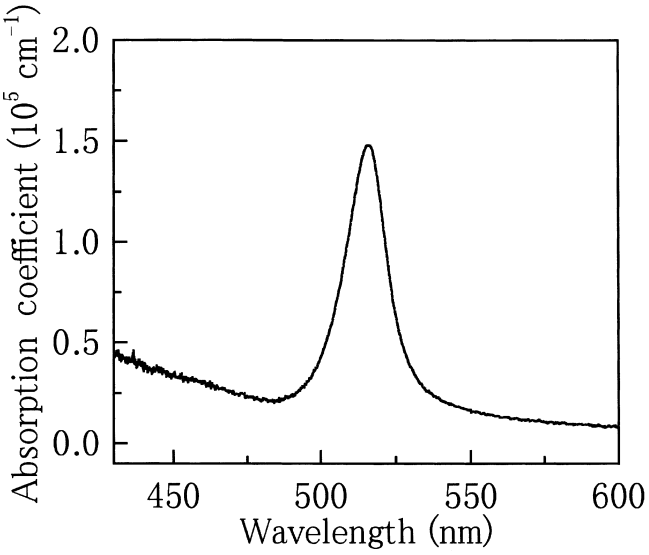

Fig. 3. Absorption spectrum of the exciton in $(C_6H_{13}NH_3)_2PbI_4$ at room temperature.

5. Experimental results

We demonstrate the time-to-space conversion with a two-pulse self-diffraction FWM configuration as shown in Fig. 4. The experiment was performed by using 300-fs optical pulses from an optical parametric amplifier seeded by an amplified mode-locked Ti:Al_2O_3 laser. The center wavelength of the pulses was tuned to the exciton resonance of $(C_6H_{13}NH_3)_2PbI_4$, 514 nm, and the spectral width of the pulses was about 4 nm which is narrower than the exciton absorption width. We produced two signal packets composed of 8-bit signals by multiplexing a single 300-fs pulse. The pulse energies of the single

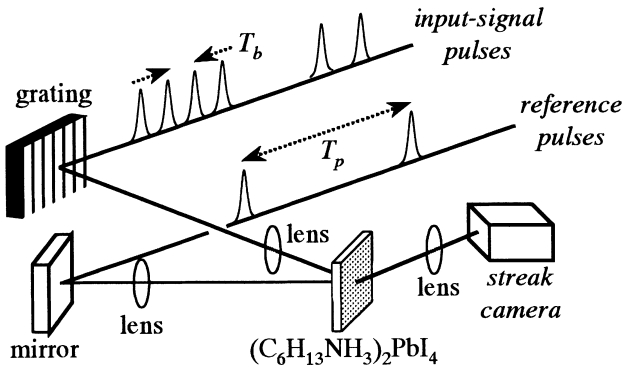

Fig. 4. Experimental setup of our serial-to-parallel conversion.

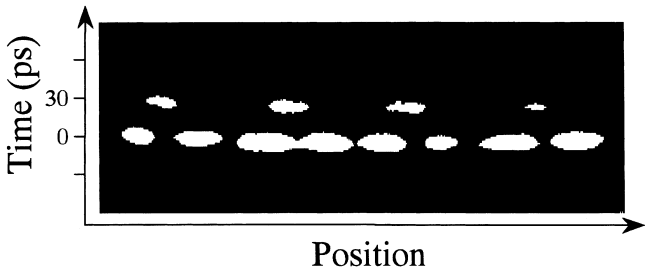

Fig. 5. An example of streak images obtained from the serial-to-parallel conversion system of Fig. 3. The image shows a spatial pattern in the x-direction and a temporal response in the y-direction.

signal pulse and the reference pulse were 1 and 60 nJ, respectively. The packet separation time T_p and the bit separation times T_b could be changed independently. The signal pulses were diffracted by a 600-lines/mm grating to project the temporal shape in the x-direction. After diffraction, the signal pulses were focused perpendicularly onto the surface of $(C_6H_{13}NH_3)_2PbI_4$ film by a lens ($f = 150$ mm) to increase incident power (not to obtain a Fourier transformation). The two synchronizing reference pulses separated by T_p were focused on the same spot of the film by a lens ($f = 500$ mm) and the spot was maintained large enough to cover the input-signal spot. The signal and reference beams lay on the same plane perpendicular to the surface of $(C_6H_{13}NH_3)_2PbI_4$. The generated FWM signals were collimated and focused onto the entrance slit of a streak camera. We confirmed the performance of our time-to-space conversion by detecting the streak images showing a spatial pattern in the x-direction and a temporal response (repetition performance) in the y-direction.

Fig. 5 shows an example of the streak images for two 8-bit packets '11111111' and '10101010' with a packet separation of 30 ps and a bit separation of 1 ps. Spatial patterns corresponding to the temporal shape of the input-signal are clearly observed. Fig. 6(a) shows a horizontal cut of the

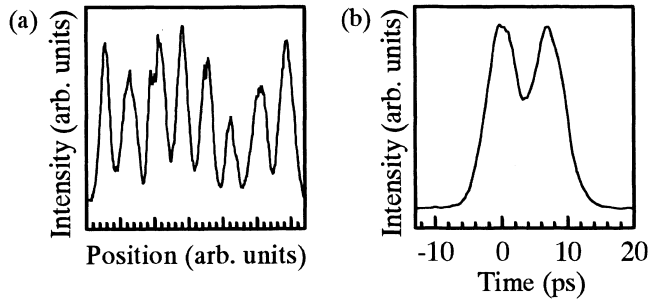

Fig. 6. (a) The horizontal cut through the streak image along the signal '11111111' and (b) the vertical cut along y-direction for $T_p = 7$ ps

streak image along the signal '11111111'. As shown in this figure, the resolution of the spatial pattern is good agreement with the expected one (Fig. 2(c)).

The response time of our system was estimated from vertical cuts of the image with reducing T_p. Fig. 6(b) shows a vertical cut of a streak image for $T_p = 7$ ps. The signals of the first and second packet are clearly separated. The figure therefore demonstrates that our system works with a conversion rate of over 140 GHz. Unfortunately, for $T_p < 7$ ps, the response time of the system was limited by the time resolution of the streak camera.

The conversion efficiency is determined by the diffraction efficiency of the FWM process, which depends on the incident power of the reference pulse. The pick-up method has higher conversion efficiency because of the higher peak power available from the reference pulse (Ishi *et al*. 2000). The conversion efficiency in our experiments is approximately 1%, which is not too large but sufficient to be detected by electronic devices.

6. Summary

We have demonstrated a simple method of a serial-to-parallel conversion. The method is based on picking up the narrow temporal range of the skewed input signal by using a nonlinear wave mixing with the reference pulse. The pick-up method has some advantages; (1) a precise alignment for Fourier transform system is unnecessary, (2) a high peak power of the reference pulse is available, and (3) a influence of relaxation times of the nonlinear material is small. We have also demonstrated our method experimentally using a self-organized quantum-well material. We have confirmed that T-bits/s pulses are clearly converted into spatial patterns with conversion rates of 140 GHz.

Acknowledgements

We thank Dr L. Boesten for the careful reading of the manuscript. This work was supported by Core Research for Evolutional Science and Technology (CREST), Japan Science and Technology Corporation (JST).

References

Boyd, R.W. *Nonlinear Optica*. Academic Press, Boston, 1992.

Butcher, P.N. and D. Cotter. *The Elements of Nonlinear Optics*. Cambridge University Press, Cambridge, 1990.

Ema, K. *Jpn. J. Appl. Phys*. **30** L2046, 1991.

Ema, K., M. Kuwata-Gonokami and F. Shimizu. *Appl. Phys. Lett.* **59** 2799, 1991.
Ema, K., T. Ogasawara, M. Kuwata-Gonokami and F. Shimizu. *Annual Report of Engineering Research Institute* **51** 103, 1992.
Hanamura, E., N. Nagaosa, M. Kumagai and T. Takagahara. *J. Material. Sci. Eng.* **1** 255, 1988.
Ishi, J., H. Kunugita, K. Ema, T. Ban and T. Kondo. *Appl. Phys. Lett.* **77** 3487, 2000.
Ishi, J., M. Mizuno, H. Kunugita, K. Ema, S. Iwamoto, S. Hayase, T. Kondo and R. Ito. *J. Nonlinear Opt. Phys. Material* **7** 153, 1998.
Ishihara, T. *In*: *Optical Properties of Low-Dimensional Materials*, T. Ogawa and Y. Kanemitsu, eds. Chap. 6. World Scientific, Singapore, 1995.
Kan'an, A.M. and A.M. Weiner. *J. Opt. Soc. Am. B* **15** 1242, 1998.
Kataoka, T., T. Kondo, R. Ito, S. Sasaki, K. Uchida and N. Miura. *Phys. Rev. B* **47** 2010, 1993.
Kondo, T., S. Iwamoto, S. Hayase, K. Tanaka, J. Ishi, M. Mizuno, K. Ema and R. Ito. *Solid State Commun.* **105** 503, 1998.
Konishi, T. and Y. Ichioka. *J. Opt. Soc. Am. A* **16** 1076, 1999.
Leaird, D.E. and A.M. Weiner. *Opt. Lett.* **24** 853, 1999.
Marinez, O.E. *Opt. Commn.* **59** 226, 1986.
Marom, D.M., D. Panasenko, P.C. Sun and Y. Fainman. *Opt. Lett.* **24** 563, 1999.
Mazurenko, Y.T., S.E. Putillin, A.G. Spiro, A.G. Beliaev, V.E. Yashin and S.A. Chizhov. *Opt. Lett.* **21** 1753, 1996.
Nuss, M.C., M. Li, T.H. Chiu, A.M. Weiner and A. Partovi. *Opt. Lett.* **19** 664, 1994.
Shimizu, F. *Jpn. J. Appl. Phys.* **26** L53, 1987.
Sun, P.C., Y.T. Mazurenko and Y. Fainman. *J. Opt. Soc. Am. A* **14** 1159, 1997.
Sun, P.C., Y.T. Mazurenko, W.S.C. Chang, P.K.L. Yu and Y. Fainman. *Opt. Lett.* **20** 1728, 1995.
Weiner, A.M. *Rev. Scientific Instruments* **71** 1929, 2000.
Weiner, A.M., D.E. Leaird, J.S. Patel and J.R. Wullert. *IEEE J. Quantum Electronics* **28** 908, 1992.